

# A Computational Framework For Robotic Quality Assessment and Management In Construction

Jingyang Liu, Yumeng Zhuang, and Joshua Bard

**Abstract**—As an integrated process in construction projects, quality assessment and management (QA&M) can be important to prevent failures during construction. The existing QA&M practice such as the evaluation of the geometric tolerance and surface qualities is mostly performed manually which can be labor-intensive and tedious. This study proposes a computational framework for a robot to perform automatic QA&M in unknown environments. The framework is composed of three parts: (1) motion planning; (2) defect detection; and (3) defect registration. The motion planning component generates efficient robotic path for autonomous exploration and surface inspection. The defect detection component quantifies surface anomalies within a user-defined area of interests through multiple sensor measurements. The defect registration component localizes the detected defects and registers the defects to a site model. To demonstrate the feasibility of the proposed framework, we present a user case for assessing geometric tolerance and surface quality of a 1500 mm (L) x 745 mm (W) x 1980 mm interior wall mockup. The result of the case study shows that the proposed framework has the potential to provide reliable geometric measurement and defect detection for gypsum wall panels in a lab environment.

## I. INTRODUCTION

Surface quality assessment and management play a key role in construction operations such as infrastructure safety monitoring, prefab component inspection, and architectural finish quality assurance. Currently, most quality assessment and management (QA&M) tasks are conducted manually by a certified inspector using a visual inspection approach or contact-type measurement devices such as measuring tapes, levels, and calipers. Manual inspection methods can be tedious, costly, and dangerous, especially when the work environment is hazardous and inaccessible. To overcome these limits, the main goal of this paper is to provide a computational framework for robots to assist humans in QA&M by (1) traversing and inspecting the area of interest on a job site where the environment may not be known a priori (2) performing remote non-contact defect detection and registration at different levels of details (LoD). The framework is composed of three components (Figure 1):

- **Motion Planning** — The motion planning component generates near-optimal paths for robots to explore the surrounding environment and scan the target area. The component integrates frontier-based and information-based methods to maximize coverage in three stage. At the first stage, the environment is unknown, the component

returns the exploration path by searching and identifying the frontier points between free and unknown parts of the map. At the second stage, a user can define a target volume within the partially known environment for detailed reconstruction, the component plans a next-best view based on the information gain of each sampled view candidate. At the third stage, a user can define an area of interest within the known environment for surface inspection. The component generates an efficient and collision-free path by minimizing the cost defined by the total traveling distance.

- **Defect Detection** — The defect detection component extracts surface anomalies and quantifies geometric tolerance based on multi-sensor measurements. The component integrates a learning-based method for recognizing components such as screws on a panel. Processing techniques including edge detection are used to detect common surface defects such as discoloration and cracks. Considering the lighting variation on construction sites, we fuse 2D images with 3D laser scanning data at decision-making level for more accurate surface anomaly detection.
- **Defect Registration** — The defect registration component registers and localizes defects in a scene model. We combine a classical ICP [1] framework and its variant Cluster ICP [2] for dense-to-dense and dense-to-sparse data registration.

This study contributes to the domain of QA&M for construction by (1) a framework for robots to explore, detect and document surface defects for construction practices. (2) expanding the surface inspection framework from a factory setting to complex unknown construction environments by introducing a three-stage autonomous exploration and reconstruction method (3) combining multi-resolution 3D reconstructions to address the discrepancies in scanning resolution and range - for instance, in construction QA&M, we need to identify surface defects at millimeter scale within a wide area at meter scale. To demonstrate the framework, we performed a surface inspection on a interior wall mockup with a 6 DoF industrial robot (Figure 2).

## II. METHOD

The framework is composed of three components: a motion planning component for generating coverage paths, a surface defect detection component for identifying and classifying surface defects at mm scale, and a defect localization component for registering and localizing defects in a scene model.

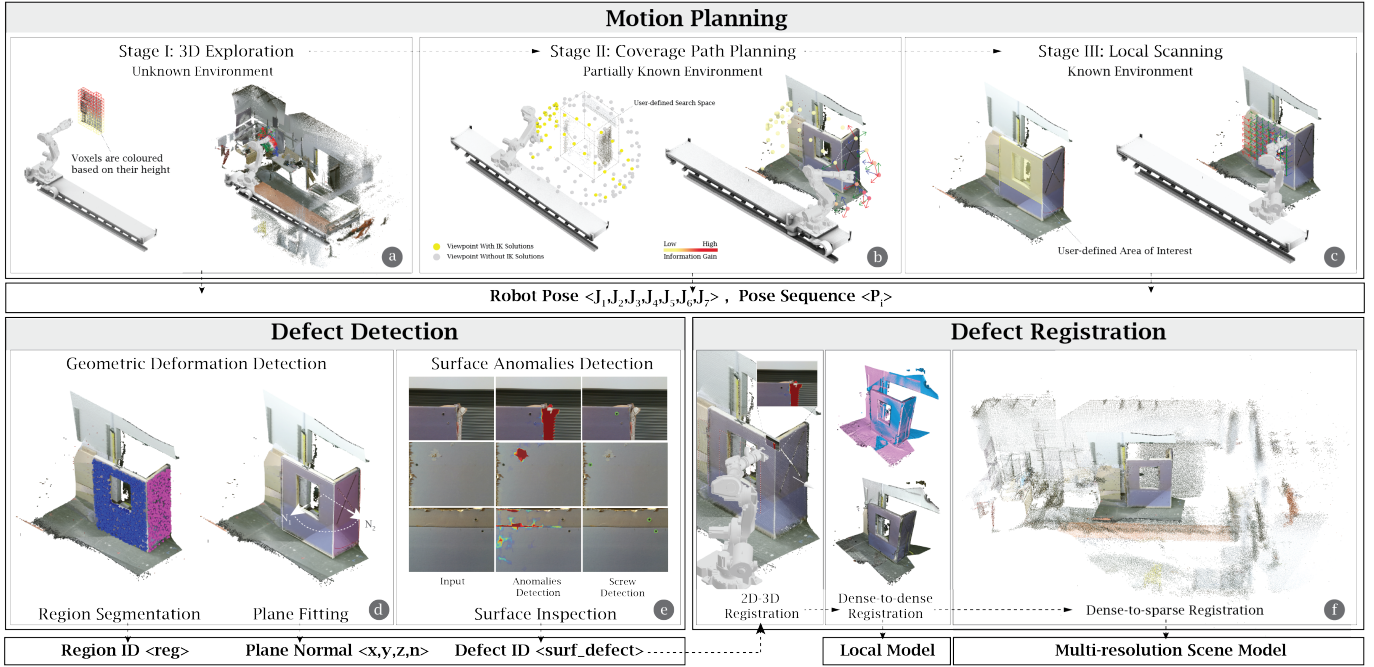


Fig. 1. The computational framework of the robotic QA&M system: (a) Frontier-based autonomous exploration in an unknown environment (b) Viewpoint generation and path planning based on information gain for covering a user-defined search space in a partially known environment (c) Local scanning path planning for covering a user-defined surface in a known environment (d) Geometric deformation detection (e) Surface anomalies detection (f) Defect registration — 2D images are registered to the target 3D surface based on known extrinsic and intrinsic parameters, local dense point clouds obtained from the same source are registered through ICP [1]. Local dense point clouds are registered to a sparse scene model through the cluster ICP framework [2].

### A. Motion Planning

The motion planning component automatically generates a collision-free path for a robot to reconstruct the site scene and inspect the user-defined areas of interest. The problem can be formulated as a coverage path planning (CPP) problem or a variant of the well-known traveling salesman problem (TSP) — an agent needs to pass over a set of target points with minimum cost (usually time or path length). However, in contrast to the traditional TSP where the environment is stationary and known a priori, in site surface inspection operations, full prior knowledge of the environment might be unrealistic. In this work, we use a three-phase approach including 3D exploration, coverage path planning, and local scanning for reconstructing a multi-resolution scene model of an unknown environment.

In the initial exploration phase, the robot explores the space by finding a set of poses along the frontier of the unknown environment and creates the occupied space map (a volumetric representation of space in a hierarchical structure). The robot first looks for a frontier located on the boundary between the explored and the unknown part of the environment, and then chooses the one with the maximum information gain weighted by its cost to reach [3] [4], which can be defined as:

$$I_f = \frac{N_0}{N} \cdot \frac{1}{|P_f - P_0|},$$

where  $I_f$  is the information gain of a candidate frontier cell.  $P_f$  and  $P_0$  represent the coordinates of the candidate frontier cell and the current pose respectively.  $N_0$  represents the unknown

voxels within a sphere of radius  $R$  around the candidate frontier that contains  $N$  voxels.

After the goal frontier is selected, the planner generates a path to move the robot 30 mm towards the frontier and look towards the direction of the frontier through an Inverse Kinematic (IK) solver unless the planner can not find a valid IK solution. The exploration procedure terminates when the void voxels within the bounded space are classified as either free or occupied.

The 3D exploration phase reconstructs a partially known scene model of the site (93.67% coverage rate) at a relatively low resolution (50 points per  $m^3$ ). Based on this model, the remote inspector can define a smaller search space for the second phase of coverage path planning. The coverage path planning aims at automatically generating collision-free robotic paths covering the required surface area within the target volume. We first combine the voxels in the volume into a binary status — “occupied” and “unoccupied” [5] [6]. The system then uniformly samples a set of viewpoint candidates on a sphere to capture the most variations of perspectives that can cover the target volume [7]. The quality of each viewpoint candidate is defined by measuring the mean entropy  $e(x)$  over all voxels within the sensor frustum of a potential next pose, which can be defined as [8] :

$$e(x) = -\frac{1}{k} \sum_{i=1}^k p_i(x) \log p_i(x) + p_i(x^c) \log p_i(x^c),$$

where  $p_i(x)$  is the probability of voxel  $x$  being occupied, and  $p_i(x^c)$  denotes the complement probability of  $p_i(x)$ ,

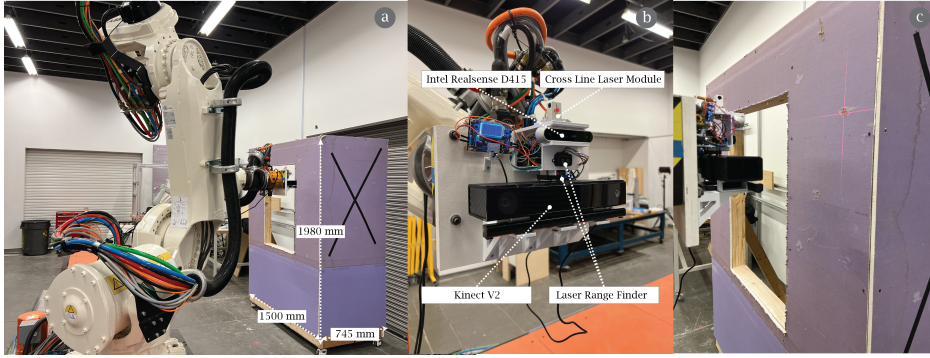


Fig. 2. Experiment setup (a) a 6 DoF industrial robot on a 5800 mm linear track and a interior wall mockup of 1500 mm (L) x 745 mm (W) x 1980 mm (H) (b) an end-effector sensor kit including RGB-D cameras (Kinect V2, Intel Realsense D415), laser range finders and a laser module (c) the robot highlights a detected surface defect with a laser cross-line.

i.e.  $p_i(x^c) = 1 - p_i(x)$ . Based on this volumetric function, we select 10 candidates with the highest visible uncertainties for coverage path planning.

After the exploration phase, we use a region-growing approach based on smoothness constraints to cluster point clouds into surface patches. The remote inspector can then choose a target surface or an area of interest on a surface for local scanning. To generate the local scanning path, we take an offline path planning algorithm formulated as an optimization process of minimizing the cost function by adjusting decision variables such as candidate viewpoints and their traversing sequence. The function is defined by the total length of robot trajectories covering the target area. An online path planning process is then integrated to address real-time adaptive motion planning to avoid collisions caused by tolerances in reconstruction.

### B. Defect Detection

Defect detection of interior wall surfaces (gypsum board) aims at identifying two types of defects — geometric deformation and surface anomalies — before finishing and painting and after the gypsum board installation. Geometric deformation can be caused by irregularities in the underlying substructure and the failure of screwing onsite. The warping of the board due to poor storage can also affect the drywall surface evenness [9]. Failures in screwing such as loosening and recession can cause surface discontinuities and result in bulges on the wall after surface finishing. Surface anomalies such as discoloration, cracks, and the detachment of the board covering can affect the aesthetics of interior wall surfaces and cause the degradation of the structure which needs to be repaired before the application of surface finishing materials.

To detect geometric deformation, we first use a principal component analysis-based approach to fit a plane within the selected point cloud. Then we can calculate the orthogonal distance between each point and the plane to evaluate surface flatness errors and calculate the connecting angle between two adjacent surfaces by computing the angle between their normal vectors.

Screwing failures need to be detected in two steps. First, screws are located based on 2D images. Their conditions are then measured using a laser range finder. To locate screws in

an image, we first detect circles with Hough circles as potential screw regions. The minimum radius and maximum radius for Hough circles are set based on the image size. We find that a minimum radius of image height divided by 150, and a maximum radius of 15 times the minimum radius work well with the Intel Realsense D415 sensor. We crop these circles as regions of interest. The regions are then classified as screw or non-screw with a fine-tuned Xception model [10]. We built our own dataset with screw pictures taken on interior wall surfaces under different lighting conditions.

Surface anomalies on gypsum boards can be visually detected by changes in color on the surface. Discoloration and cracks often have clear boundaries and/or rougher texture than the normal areas. We apply Contrast Limited Adaptive Histogram Equalization (CLAHE) to blurred images to reduce the effect of lighting changes. Then we extract edges with a Canny edge detector, and use morphological operations to cover the regions with dense edges, which correspond to the rougher texture of surface anomalies. We also use the depth information to discard the pixels with depth greater than 50 cm, since they are not on the wall. With the remaining regions, we filter out the regions with contour areas greater than one standard deviation above average and classify them as surface anomalies. We also notice that surface anomaly detection and screw detection work optimally at different distances from the gypsum board.

As construction sites can be affected by complex and unpredictable lighting environments, to compensate for illumination variations and shadows, we combine both 2D and 3D data for defect detection. 2D image processing can extract the potential defects in images. 3D geometric information is used for detecting volumetric defects defined by sharp changes in a depth reading. Depth reading is acquired by a fusion of a stereo camera and laser range finder to compensate for each individual sensor's deficiencies — stereo vision can produce dense output but performs poorly on textureless surfaces or regions with repetitive patterns, and the data collected from the laser range finder is accurate but relatively sparse in nature [11]. The extracted defects from 2D and 3D data are fused at the decision-making level based on evidence theory — a general framework for modeling epistemic uncertainty for multi-sensor fusion.

### C. Defect Registration

The detected surface defects need to be registered to a site scene model, an inspector can thus localize the surface defects and authorize surface repair tasks. The registration process is completed in two phases - common source registration and cross-source registration. During common source registration, we first register the detected defects to a point cloud paired with the current robot pose and then fuse the point cloud acquired between different robot poses into a local model. The detected defects are registered to a point cloud by applying the transform matrix that is known after sensor calibration. We then use the Iterative Closest Point (ICP) algorithm for point cloud registration between frames. Since the local model and site scene model are of large discrepancies in densities, the registration method based on classical ICP may yield inaccurate pose estimation. To address the cross-source registration issue, we used the clustering iterative closest point (CICP) approach [2]. CICP integrates a novel correspondence point selection process based on voxelization and clustering before the matching. Each selected point can represent a local surface in a voxel of the source and target point clouds. Based on the selected correspondence points, the matching process is invariant to the point cloud density and scanning pattern. After the two-phase registration, defects and robots can share a common world-locked coordinate system for the user to reference.

### III. RESULT

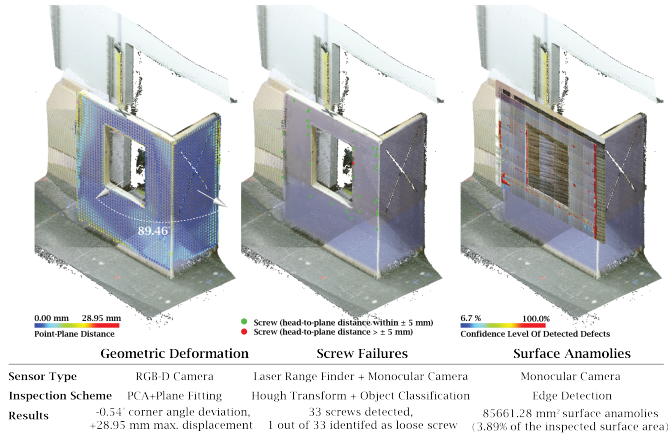


Fig. 3. The robotic quality assessment result of the interior wall mockup

To validate the proposed framework, we conducted a lab experiment using a 6 DoF industrial robot mounted on a linear track for surface inspection of an L-shaped mock-up wall in the dimension of  $1500\text{mm}(L) \times 745\text{mm}(W) \times 1980\text{mm}$ . We used a Kinect V2 sensor for 3D exploration and a combination of Intel RealSense D415 Sensor and laser range finders for the detection of surface anomalies. According to the surface inspection results (Figure 3), the mockup wall has 8.18% area identified as not flat (deviation from the fitted plane  $> 10$  mm). The maximum displacement on the drywall is 28.95 mm. The angle between the two surfaces is  $-0.54$  degrees deviating from the expected angle (90 degrees). The total

area of surface anomalies is  $85661.28\text{ mm}^2$ , accounting for 3.86% of the total surface area. 1 out of 33 of screws detected is identified as loose. To further optimize the framework, the potential focus could be on (1) a more efficient 3D exploration process: the existing framework examines every cell in the robot's map to trace the frontier for a next move. With the increase of searching space, the frontier evaluation process can be computationally inefficient. A faster frontier detection algorithm such as [12] or an active sub-map with bounded space can potentially improve the performance of 3D exploration. (2) a more robust view planning algorithm: job sites can be cluttered and dynamic which may result in occlusion. The compensation of occlusion adaptive to dynamic scenes can be integrated into the view planning process to avoid failures in coverage requirements. (3) a more accurate registration process: the discrepancies between the scale of the site and the scale of defects in construction practices can be large. A multi-resolution 3D reconstruction is efficient for capturing high resolution details of selected areas within a wide range space. As the density difference, scale variation, and noises from different types of sensors can pose challenges to the accuracy of point cloud fusion, optimization in transformation estimation between cross-source 3D data can be further explored in future work.

### REFERENCES

- [1] P. J. Besl and N. D. McKay, "Method for registration of 3-D shapes," in *Sensor fusion IV: control paradigms and data structures*, vol. 1611, 1992, pp. 586–606.
- [2] M. L. Tazir, T. Gokhool, P. Checchin, L. Malaterre, and L. Trassoudaine, "CICP: Cluster Iterative Closest Point for sparse-dense point cloud registration," *Robotics and Autonomous Systems*, vol. 108, pp. 66–86, 2018.
- [3] C. Zhu, R. Ding, M. Lin, and Y. Wu, "A 3d frontier-based exploration tool for mavs," in *2015 IEEE 27th International Conference on Tools with Artificial Intelligence (ICTAI)*, 2015, pp. 348–352.
- [4] L. Lu, C. Redondo, and P. Campoy, "Optimal frontier-based autonomous exploration in unconstructed environment using RGB-D sensor," *Sensors*, vol. 20, no. 22, p. 6507, 2020.
- [5] J. I. Vasquez-Gomez, L. E. Sucar, R. Murrieta-Cid, and E. Lopez-Damian, "Volumetric next-best-view planning for 3D object reconstruction with positioning error," *International Journal of Advanced Robotic Systems*, vol. 11, no. 10, p. 159, 2014.
- [6] P. S. Blaer and P. K. Allen, "Data acquisition and view planning for 3-D modeling tasks," in *2007 IEEE/RSJ International Conference on Intelligent Robots and Systems*, 2007, pp. 417–422.
- [7] S. Isler, R. Sabzevari, J. Delmerico, and D. Scaramuzza, "An information gain formulation for active volumetric 3D reconstruction," in *2016 IEEE International Conference on Robotics and Automation (ICRA)*, 2016, pp. 3477–3484.
- [8] J. Daudelin and M. Campbell, "An adaptable, probabilistic, next-best view algorithm for reconstruction of unknown 3-d objects," *IEEE Robotics and Automation Letters*, vol. 2, no. 3, pp. 1540–1547, 2017.
- [9] C. Gaião, J. de Brito, and J. Silvestre, "Inspection and diagnosis of gypsum plasterboard walls," *Journal of Performance of Constructed Facilities*, vol. 25, no. 3, pp. 172–180, 2011.
- [10] E. Yildiz and F. Wörgötter, "Dcnn-based screw detection for automated disassembly processes," in *2019 15th International Conference on Signal-Image Technology & Internet-Based Systems (SITIS)*, 2019, pp. 187–192.
- [11] D. Huber and T. Kanade, "Integrating lidar into stereo for fast and improved disparity computation," in *2011 International Conference on 3D Imaging, Modeling, Processing, Visualization and Transmission*, 2011, pp. 405–412.
- [12] M. Keidar and G. A. Kaminka, "Efficient frontier detection for robot exploration," *The International Journal of Robotics Research*, vol. 33, no. 2, pp. 215–236, 2014.